Dopant diameter dependence of $J_{\mathrm{C}}(B)$ in doped YBCO films

P. Paturi, M. Malmivirta, H. Palonen and H. Huhtinen

***Abstract*—In YBCO films doped with artificial pinning centers, such as $BaZrO_3$ nanorods or $BaCeO_3$ nanodots, the critical current density, $J_c(B \parallel c)$, is usually described with the form $J_c \sim B^{-\alpha}$ even though the shape of the $J_c(B)$-curve does not really allow this. In the field region just above the low field plateau, the shape of the $J_c(B)$-curve (in log-log scale) is rounded and not straight as in undoped films. The exponent α is found to decrease from 0.5 to around 0.2 in $BaZrO_3$ doped films and to 0.4 in $BaCeO_3$ doped films. The incompatibility with the curved data and the linear fit has lead to publication of α-parameters which are not comparable to each other due to different fitting limits. In this paper we show that it is better to use the Dew-Hughes pinning force $F_p(B) = F_{p0}(B/B_{\mathrm{irr}})^p(1-B/B_{\mathrm{irr}})^q$ to describe the field dependence, where $\alpha \approx 1-p$. We also show that the p and the roundness of the curve depend on the diameter of the pinning centers, but not e.g. temperature or dopant concentration. This is shown from measurements of differently doped thin YBCO films and from large scale Ginzburg-Landau simulations. The result should have been expected since the diameters of the dopants are roughly the same size as the coherence length and it has been shown earlier that pinning centers much smaller than the coherence length lead to $\alpha = 0.5$ and those much larger lead to $\alpha = 1$.**

***Index Terms*—YBCO thin films, flux pinning, artificial pinning sites, pinning force**

I. Introduction

In applications of high temperature superconductors one of the most important properties is the dependence of critical current density on magnetic field, $J_c(B)$. In high temperature superconductors, specifically $YBa_2Cu_3O_{6+x}$ (YBCO), J_c typically decreases fast above magnetic field around 100 mT [1]. This decrease is due to insufficient pinning of the magnetic vortices in high fields. Adding artificial pinning centers (APC), such as $BaZrO_3$ [2], [3] or $BaSnO_3$ nanorods [4] or *e.g.* Y_2O_3 [5] or $BaCeO_3$ [6] nanodots, increases pinning, and thus J_c at high fields.

In the description of $J_c(B \parallel c)$ dependence on magnetic field, the common practice [1], [3] is to define parameter α from $J_c \propto B^{-\alpha}$ fits to $J_c(B)$ data, even though most of the APC-film data does not follow this dependence. The practice arises from the undoped films, which on log-log scale have a clear linear part of the $J_c(B)$-curve and determination of α is straightforward. This linear dependence is also well supported by theory [7]. In APC-films there is no such linear part and the problem arises from defining the fitting limits. The end of the low field plateau of J_c is not well defined and the determination of B^* as the field where the plateau ends and where the fit should start is difficult or even impossible. In undoped films the most used definition of B^* is $J_c(B^*) = 0.9J_c(0)$ as suggested by Klaassen *et al.* [1]. This problem is even more pronounced at high temperatures and the arbitrariness of α definition makes comparison of films from different groups difficult or impossible.

Analysis of the $J_c(B)$-curves is not a novel topic, many summation theories have been presented ever since the seminal models by Dew-Hughes [8] and Kramer [9]. A good presentation of all the main theories has been done by Matsushita in [10]. The general form of the function describing the pinning force $\mathbf{F_p} = \mathbf{B} \times \mathbf{J_c}$ in these theories is

$$F_p(B) = F_{p0}\left(\frac{B}{B_{c2}}\right)^p\left(1-\frac{B}{B_{c2}}\right)^q, \qquad (1)$$

where F_{p0} is the pinning force at $B = 0$, B_{c2} is the upper critical field and p and q are exponents which depend on the type of pinning sites in the sample. In the model by Dew-Hughes for non-magnetic pinning sites, if the diameter d is much smaller than the coherence length ξ, $p = 0.5$ and if $d \gg \xi$, $p = 1$. The parameter $q = 2$ if the pinning sites are non-superconducting and 1 if they are superconductors with smaller $T_{c,\mathrm{onset}}$, B_c, or κ ($\Delta\kappa$ pinning). Even though Dew-Hughes meant for the exponents p and q to be constants, they are generally used as fitting parameters [10]. In high-temperature superconductors B_c has been replaced by B_{irr} [11], as in them B_{irr} marks the limit above which J_c is zero. A few papers have also tried to understand pinning based on sum of different contributions [12], [13].

In this paper we show that using the suitably scaled pinning force function for fitting F_p, the films from different research groups can be better compared. We also show that the size of the pinning centers affects the exponents in Eq. (1).

II. Experimental details and methods

The YBCO films used in this work were deposited on single crystal $SrTiO_3$ (100) (STO) substrates by pulsed laser deposition (PLD) at 750 °C. Details of the deposition are found elsewhere [14]. The $BaZrO_3$ (BZO) doped targets used for the films were prepared using the sol-gel method with concetrations of BZO varying from 0 – 9 % [15]. The same films have been earlier used in [16]. Also a series of 5 % BZO doped samples deposited at different temperatures were used, these films have been used before in [17]. The sizes of

Manuscript received August 31, 2015. This work is supported by the Jenny and Antti Wihuri Foundation.

P. Paturi, M. Malmivirta and H. Huhtinen are with the Wihuri Physical Laboratory, Department of Physics and Astronomy, University of Turku, FI-20014 Turku, Finland.

H. Palonen is with Department of Physics and Astronomy, Uppsala University, SE-752 37 Uppsala, Sweden

the BZO nanorods have also been determined by transmission electron microscopy (TEM) earlier [3], [17]. The $BaCeO_3$ (BCO) doped targets were prepared by the solid state method with 0, 2, 4 and 8 % concentrations. The same films have been used before in [6]. BCO grows as epitaxial nanoparticles into the YBCO lattice and the sizes of the BCO nanodots have been determined by TEM [6].

The critical current densities of the films were determined from hysteresis loops measured with a Quantum Design PPMS magnetometer and using the Bean formula for thin films [18]. The planes of the films were always perpendicular to the magnetic field, making the determination of the pinning force easy: $F_{\rm p}(B)$= $BJ_{\rm c}(B)$. The measurements were done between -8 – 8 T at temperatures 10 – 80 K.

III. Results

A. Experimental results

The fitting of the $F_{\rm p}(B)$ was done by first scaling the data by $F_{\rm p,max}$ and $B_{\rm max}$, so that the maximum of the $F_{\rm p}(B)$ plot was at (1,1). This makes the comparison of the films much easier. The maximum values were chosen, because in most cases it was not possible to determine $B_{\rm irr}$ accurately. In this case, Eq. (1) changes to

$$\begin{aligned}\frac{F_{\rm p}(B)}{F_{\rm p,max}} &= \frac{(p+q)^{p+q}}{p^p q^q}\left(\frac{B}{B_{\rm max}}\frac{p}{p+q}\right)^p\left(1-\frac{B}{B_{\rm max}}\frac{p}{p+q}\right)^q \\ &= \frac{(p+q)^{p-1}p^q}{q^q}\left(\frac{B}{B_{\rm max}}\right)^p\left(\frac{p+q}{p}-\frac{B}{B_{\rm max}}\right)^q\end{aligned} \quad (2)$$

This has the advantage of having only two free parameters after scaling with the maximum values. Fig. 1 shows examples of the fits for samples with different kinds of pinning sites: dislocations for undoped, nanorods for BZO-doped and nanodots for BCO-doped films. It can be clearly seen that the Eq. (2) fits the data well above B^*, which was used as the lower limit for the fit. Specifically in the case of the BZO-doped film, the $J_{\rm c}(B)$ curve (inset of Fig. 1) is very round and fitting a straight line would be tedious and prone to errors. It is also seen that the three films clearly have different p-values, which corresponds, as a first order estimate, to the usual α as $\alpha = 1 - p$ as can be seen from the low B limit of Eq. (1), where the second term is zero and $F_{\rm p}$= $BJ_{\rm c}\sim$ $B^{1-\alpha}$. The obtained p, q, $B_{\rm max}$and $F_{\rm p,max}$values are listed in Table I.

To get confirmation of the q values obtained from the pinning force fits, the $F_{\rm p}$ data of the 4 % BZO-doped film sample at different temperatures were plotted together and temperature scaling was confirmed (Fig. 2). This was expected, since it is widely used in low temperature superconductors [10]. As can be seen, the p- and q-values do not depend on temperature and thus single values can be used for each sample. The obtained best fit q for the 4 % BZO-film was 1.1, which is shown in the figure. The value is in between the values given by most theories [10] or by Dew-Hughes [19] for normal pinning ($q = 2$) and $\Delta\kappa$ pinning ($q = 1$). Eq. (2) with $q = 2$ is also plotted in Fig. 2 to illustrate that the value of q has a clear effect on the line shape. The obtained q values for all the films are shown in Table I, all values were

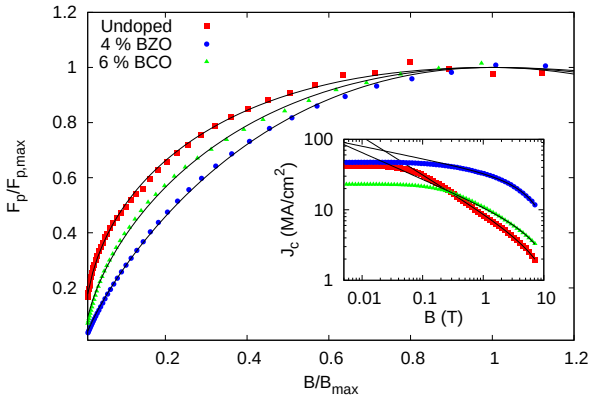

Fig. 1. Examples of fits of Eq. (2) to $F_{\rm p}$ data of undoped, 4 % BZO-doped and 6 % BCO-doped films at 10 K. The inset shows the original $J_{\rm c}(B)$ data with the same fits.

TABLE I
THE OBTAINED FITTING PARAMETERS, p, q, $B_{\rm max}$(10 K) AND $F_{\rm p,max}$(10 K) FOR ALL THE FILMS, TOGETHER WITH THE DIAMETERS OF THE MAIN PINNING SITES IN THE FILMS.

Sample	d (nm)	p	q	$B_{\rm max}$(T)	$F_{\rm p,max}$(GN/m^3)
Undoped	0.3	0.48	1.09	5.68	141.93
BZO-2.6 %	5	0.81	1.09	6.16	826.29
BZO-4 %	5	0.81	1.09	6.56	839.73
BZO-5 %	5	0.82	1.10	7.66	938.75
BZO-7.5 %	5	0.87	1.10	5.41	612.53
BZO-9%	5	0.82	1.10	11.12	656.80
BZO-700	5	0.81	1.09	6.18	84.28
BZO-725	5	0.81	1.10	11.31	785.41
BZO-775	6.5	0.88	1.07	7.35	1112.72
BZO-825	12.5	0.91	1.07	5.71	931.07
Undoped	0.3	0.50	1.10	7.78	209.43
BCO-2 %	1.6	0.56	1.09	8.16	297.18
BCO-4 %	2.5	0.60	1.11	7.77	309.13
BCO-8 %	3.6	0.70	1.11	5.10	201.25

very close to 1.1. It is obvious from Fig. 2 that the Eq. (2) is not optimal for these samples at high temperatures. There is a long tail at high magnetic field, which is not well fitted by this function with any q. This has been remedied in some papers by using an additional exponential term in the fitting equation [11], [20]. Since we are mostly interested in the rising part of the function and at high temperature flux creep has a significant effect which cannot be scaled with Eq. (1), we chose to be content with the fits similar to that shown in Fig. 2

B. Simulation results

The simulation of the flux pinning was made by solving the Ginzburg-Landau equations using a computational model described in [21]. In the model, pinning sites are introduced by locally restricting the maximum possible value of the order parameter ψ. Thus, the total energy decreases when the vortices are located in the pinning sites. For computational reasons the simulation works in dimensionless energies and the only lengthscale is the magnetic penetration depth, which

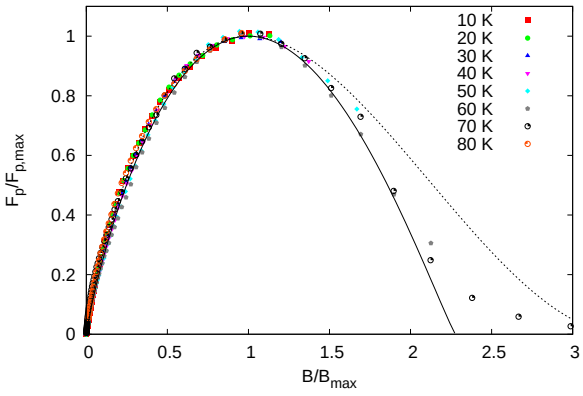

Fig. 2. Temperature scaling of the F_p of the 4 % BZO-doped sample. The black line is the scaled $F_\mathrm{p}(B)$ with $p = 0.81$ and $q = 1.1$. The dashed line shows the $F_\mathrm{p}(B)$ with $q = 2$.

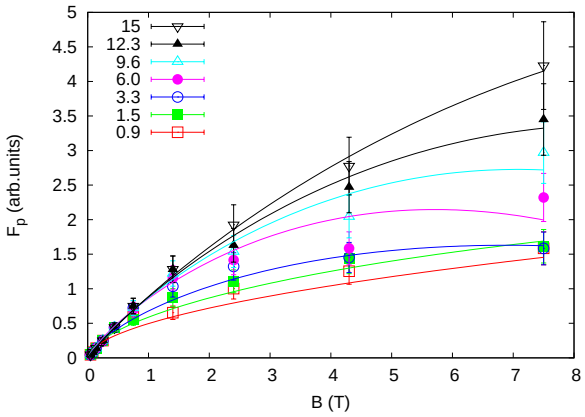

Fig. 3. Pinning force from the Ginzburg-Landau simulation together with fits to Eq. (2). The legend gives pinning center diameters in nanometers. The sizes were scaled from the original simulation with ξ so that they correspond directly to those in the experimental data.

was chosen to be $\lambda = 1$ and therefore the coherence length $\xi = 1/\kappa$, where κ is the Ginzburg-Landau parameter. For YBCO $\kappa \approx 100$ [22]. In ref. [21] it was shown that the calculation can be done with $\kappa = 10$ without loosing accuracy. The diameters of the pinning centers were determined in proportion to ξ (for YBCO $\xi = 1.5$ nm [22]) and were chosen so that they cover the whole experimental range observed in YBCO films. The critical current density was determined from the proportion of the pinned vortices to all vortices present. This does not give us absolute J_c values, but rather the dependence of J_c on B, which is what we need in this case. The simulated $J_\mathrm{c}(B)$ values used in this work have been published earlier in [21].

Results of the simulation are shown in Fig 3. Errors, shown with errorbars, are estimated to be 15 % as in the other simulations [21]. The errors are mostly due to the random positions of the pinning sites, which lead to different J_c values. The fits to Eq. (2) were made taking into account the estimated errors and are also shown in Fig. 3. The obtained q values were very close to 1.1 as in the experimental data and the p values varied from 0.5 to 0.91, which agree well with the experimental data.

IV. Discussion

The p's obtained from the fits for all the samples and the simulations as function of the known pinning site diameter are shown in Fig. 4. The mean sizes of the pinning sites have been determined by TEM earlier [3], [6], [17] and are listed in Table I together with the p, q, $F_\mathrm{p,max}$ and B_max values obtained from the fits. The sizes referred here are the diameters perpendicular to the magnetic field.

It is clearly seen from Fig. 4 that all the values fall onto the same dependence. At low pinning site sizes $p \approx 0.5$ as predicted for small pinning sites for which $d \ll \xi$ [8]. From there p increases with pinning site size until the tendency changes around $d \approx 6$ nm ($r \approx 2\xi$). Similar increase of p with nanorods has been reported *e.g.* in [23], where p = 0.7 was observed for 4-5 nm nanorods, in accordance with the data here. Above 6 nm $p \approx 0.9$ for all pinning site sizes. This is close to $p = 1$ describing constant $J_\mathrm{c}(B)$ (as a first approximation $\alpha = 0$) and the result predicted by the early papers for pinning by large precipitates [8]. In these samples the main roundness of the $J_\mathrm{c}(B)$ curve comes from the second term of Eq. (2) (described by q), which is mostly determined by the elastic properties of the flux line lattice. This limit is at the same pinning site size above which the simulations show several vortices per pinning site, *i.e.* multivortices [21]. It should be noted that the main determining factor here is the pinning site diameter, not the density. If the density of the pinning sites was the determining factor, the BZO concetration series should have different p values, as in that series the diameter does not change [3]. Also, we emphasize that this analysis is done on films with $B \parallel c$. In other directions the sizes of the pinning sites and exponents would be different.

Ginzburg-Landau theory provides a fairly simple way of arriving to Eq. (1) with small and large pinning sites, without the need to go into the complicated determination of the elastic constants of the vortex lattice. The condensation energy per unit length of a vortex is $E = \pi\mu_0 H_c^2 \xi^2$, where H_c is the thermodynamic critical field. If the vortex core is located in a pinning site where the superconductivity is locally depressed, some of this energy can be recovered (the core interaction). If the vortex sits on a small defect with volume V, the maximum pinning energy is [24]

$$U_0 = \frac{3}{2}\mu_0 H_c^2 V \frac{\delta H_{c2}}{H_{c2}} \langle |\frac{\psi}{\psi_0}|^2 \rangle, \qquad (3)$$

where H_{c2} is the upper critical field and $|\psi/\psi_0|^2 = 1 - B/B_{c2} = 1 - b$ is the variation of the order parameter. If the pinning force is so small that the vortex lattice stays almost intact, the maximum pinning force is $\pi U_0/a_0$ [25], where $a_0 \propto \sqrt{\phi_0/B}$ is the average distance between the vortices.

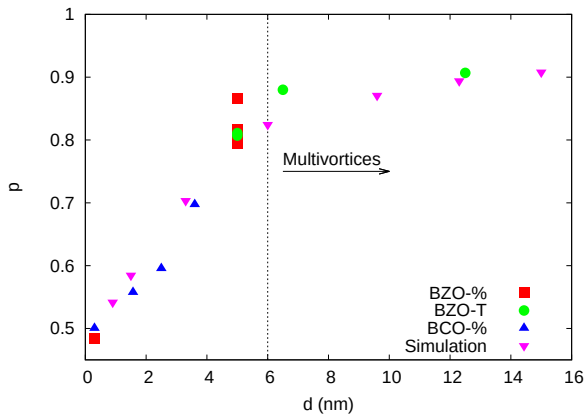

Fig. 4. The fitted p values as function of the diameter of the dominating pinning site. BZO-% refers to the BZO concentration series, BZO-T to the deposition temperature series and BCO-% to the BCO concentrations series. The dashed line shows the limit above which the simulations showed multiple vortices per pinning center.

This leads to

$$F_\mathrm{p} \propto b^{1/2}(1-b) \qquad d \ll \xi \tag{4}$$

dependence, which is observed here for dislocations in the undoped sample.

In the case, when the vortex lattice does not stay intact, *i.e.* with strong pinning, direct summation of the pinning force can be used [26], [27]. The total pinning force is therefore [25]

$$F_\mathrm{p} \approx f_p N \propto b(1-b) \qquad d \gg \xi, \tag{5}$$

where N is the number of pinned vortices, which is assumed to be directly proportional to the magnetic field, since the pinning sites are so dense that all the vortices are pinned. The maximum pinning force, f_p can be estimated from Eq. (3) by dividing by the characteristic length scale of the change in the order parameter, *i.e.* ξ. If the pinning sites would be dilute N would be the number density of the pinning sites. This region has been called the core pinning region in many references, *e.g.* [28] and is typically observed in NbTi samples, where the pinning sites are nonsuperconducting α-Ti inclusions. These are morphologically similar to the artificial pinning sites in the current films.

It is intuitive that p cannot change abruptly from 0.5 to 1 when the size of the pinning site increases, instead there should be a gradual change when $d \approx \xi$. Also according to the simulations [21], the vortex lattice smoothly distorts when the size of the pinning sites is increased and no abrupt changes are observed. Therefore the gradual change of p from 0.5 to 1 is supported by the Ginzburg-Landau theory. To our knowledge actual calculation in this range has not been performed.

Next, we turn to the high field region, which is mostly described by q. In this region, the repulsive vortex-vortex interaction begins to be the main determining factor. Above we have arrived to $q = 1$ from Ginzburg-Landau considerations of core pinning, but other derivations often lead to $q = 2$ [10], [24], [27]. These are mostly based on deriving the shear elastic modulus c_{66} of the vortex lattice. Also other, more complicated forms have been presented, *e.g.* in [20]. It has also been stated that the statistical variation of the pinning sites' strength can change the q drastically and even lead to misinterpretations of the pinning process [28]. The values for q obtained here differ only slightly from 1, which can probably be accounted by the statistical variation of pinning site sizes, which has been observed in TEM images.

Pinning mechanisms are often judged on the position of the maximum of F_p in the B/B_irr scale. Using Eq. (2) one gets that the maximum of F_p occurs at $B_\mathrm{max}/B_\mathrm{irr} = p/(q+p)$, which varies from 0.3 to 0.5 in the samples here. Since q is almost constant, the dependence of the position of $F_\mathrm{p,max}$on pinning site size is almost identical to Fig. 4. This indicates a similar gradual change in pinning mechanism as described above from the p values.

V. Conclusions

In this paper we have shown that using pinning force fitting, the magnetic field dependences of critical current densities of high-temperature superconductors with artificial pinning sites, can be described much better than with the more usual $J_\mathrm{c} \propto B^{-\alpha}$ fitting. Pure YBCO samples and samples with $BaZrO_3$ and $BaCeO_3$ inclusions, as well as results from Ginzburg-Landau simulations were analysed using this method. It was found that the obtained p values clearly depend on the diameter of the pinning sites. Dependence on the density of the pinning sites could be excluded.

The obtained limiting values for p were found to be those obtained from the Ginzburg-Landau theory, and the values in between correlated very well with the breaking of the vortex lattice when the pinning site size is increased.

References

[1] F. C. Klaassen, G. Doornbos, J. M. Huijbregtse, R. C. F. van der Geest, B. Dam, and R. Griessen, "Vortex pinning by natural linear defects in thin films of $YBa_2Cu_3O_{7-\delta}$," *Phys. Rev. B*, vol. 64, p. 184523, 2001.

[2] J. L. MacManus-Driscoll, S. R. Foltyn, Q. X. Jia, H. Wang, A. Serquis, L. Civale, B. Maiorov, M. E. Hawley, M. P. Maley, and D. E. Peterson, "Strongly enhanced current densities in superconducting coated conductors of $YBa_2Cu_3O_{7-x}$ + $BaZrO_3$," *Nat. Mater.*, vol. 3, p. 439, 2004.

[3] M. Peurla, P. Paturi, Y. P. Stepanov, H. Huhtinen, Y. Y. Tse, A. C. Bódi, J. Raittila, and R. Laiho, "Optimization of the $BaZrO_3$ concentration in YBCO films prepared by pulsed laser deposition," *Supercond. Sci. Technol.*, vol. 19, pp. 767–771, 2006.

[4] P. Mele, K. Matsumoto, A. Ichinose, M. Kukaida, Y. Yoshida, S. Horii, and R. Kita, "Systematic study of the $BaSnO_3$ insertion effect on the properties of $YBa_2Cu_3O_{7-x}$ films prepared by pulsed laser ablation," *Supercond. Sci. Technol.*, vol. 21, p. 125017, 2008.

[5] K. Matsumoto, T. Horide, K. Osamura, M. Mukaida, Y. Yoshida, A. Ichinose, and S. Horii, "Enhancement of critical current density of YBCO films by introduction of artificial pinning centers due to the distributed nano-scaled Y_2O_3 islands on substrates," *Physica C*, vol. 412-414, p. 1267, 2004.

[6] M. Malmivirta, L. Yao, S. Inkinen, H. Huhtinen, H. Palonen, R. Jha, V. P. S. Awana, S. van Dijken, and P. Paturi, "The angular dependence of critical current of $BaCeO_3$ doped $YBa_2Cu_3O_{6+x}$ thin films," *IEEE T. Appl. Supercond.*, vol. 25, p. 6603305, 2015.

[7] G. Blatter, M. Feigel'man, V. Geshkenbein, A. Larkin, and V. Vinokur, "Vortices in high-temperature superconductors," *Rev. Mod. Phys.*, vol. 66, p. 1125, 1994.

[8] D. Dew-Hughes, "Flux pinning mechanisms in type ii superconductors," *Philosophical magazine*, vol. 30, p. 293, 1974.

[9] E. J. Kramer, "Scaling laws for flux pinning in hard superconductors," *J. Appl. Phys.*, vol. 44, p. 1360, 1973.

[10] T. Matsushita, *Flux pinning in superconductors*. Springer, Heidelberg, Germany, 2007.

[11] S. N. Barilo, S. V. Shiryaev, V. I. Gatalskaya, J. W. Lynn, M. Baran, H. Szymczak, R. Szymczak, and D. Dew-Hughes, "Scaling of magnetization and some basic parameters of $Ba_{1-x}K_xBiO_{3-y}$ superconductors near T_c," *Phys. Rev. B*, vol. 58, p. 12355, 1998.

[12] A. Crisan, V. S. Dang, G. Yearwood, P. Mikheenko, H. Huhtinen, and P. Paturi, "Investigation of the bulk pinning force in YBCO superconducting films with nano-engineered pinning centres," *Physica C*, vol. 503, p. 89, 2014.

[13] R. Ma, Y. Ma, W. Song, X. Zhu, S. Liu, J. Du, Y. Sun, C. Li, P. Ji, Y. Feng, and P. Zhang, "Imperfection of flux pinning classification based on the pinning center size," *Physica C*, vol. 411, p. 77, 2004.

[14] H. Palonen, H. Huhtinen, M. A. Shakhov, and P. Paturi, "Electron mass anisotropy of $BaZrO_3$ doped YBCO thin films in pulsed magnetic fields up to 30 T," *Supercond. Sci. Technol.*, vol. 26, p. 045003, 2013.

[15] J. Raittila, H. Huhtinen, P. Paturi, and Y. P. Stepanov, "Preparation of superconducting $YBa_2Cu_3O_{7-\delta}$ nanopowder by deoxydation in Ar before final oxygenation," *Physica C*, vol. 371, pp. 90–96, 2002.

[16] H. Huhtinen, M. Irjala, P. Paturi, M. A. Shakhov, and R. Laiho, "Influence of $BaZrO_3$ dopant concentration on properties of $YBa_2Cu_3O_{6+x}$ films in magnetic fields up to 30 T," *J. Appl. Phys.*, vol. 107, p. 053906, 2010.

[17] M. Malmivirta, L. Yao, H. Huhtinen, H. Palonen, S. van Dijken, and P. Paturi, "Three ranges of the angular dependence of cirtical current of $BaZrO_3$ doped $YBa_2Cu_3O_{7-\delta}$ thin films grown at different temperatures," *Thin Solid Films*, vol. 562, pp. 554–560, 2014.

[18] H. P. Wiesinger, F. M. Sauerzopf, and H. W. Weber, "On the calculation of J_c from magnetization measurements on superconductors," *Physica C*, vol. 203, pp. 121–128, 1992.

[19] D. Dew-Hughes, "The critical current of superconductors: an historical review," *Supercond. Sci. Technol.*, vol. 27, p. 713, 2001.

[20] E. H. Brandt, "Range and strength of pins collectively interacting with the flux-line lattice in type-II superconductors," *Phys. Rev. Lett.*, vol. 57, p. 1347, 1986.

[21] H. Palonen, J. Jäykkä, and P. Paturi, "Modeling reduced field dependence of critical current density in $YBa_2Cu_3O_{6+x}$ films with nanorods," *Phys. Rev. B*, vol. 85, p. 024510, 2012.

[22] G. Blatter, M. V. Feigel'man, V. B. Geshkenbein, A. I. Larkin, and V. M. Vinokur, "Vortices in high-temperature superconductors," *Reviews of Modern Physics*, vol. 66, pp. 1125–1388, 1994.

[23] T. Matsushita, H. Nagamizu, K. Tanabe, M. Kiuchi, E. S. Otabe, H. Tobita, M. Yoshizumi, T. Izumi, Y. Shiohara, D. Yokoe, T. Kato, and T. Hirayama, "Improvement of flux pinning performance at high magnetic fields in $GdBa_2Cu_3O_y$ coated conductors with BHO nanorods through enhancement of B_{c2}," *Supercond. Sci. Technol.*, vol. 25, p. 125003, 2012.

[24] H. Ullmaier, *Irreversible properties of type II superconductors*. Springer-Verlag Berlin Heidelberg, 1975.

[25] A. M. Campbell and J. E. Evetts, "Flux vortices and transport currents in type II superconductors," *Adv. Phys.*, vol. 21, p. 199, 1972.

[26] V. I. Dedyu, A. N. Lykov, and S. L. Prishchepa, "Critical currents in niobium-based layer structures," *Sov. Phys. JETP*, vol. 70, p. 488, 1990.

[27] E. H. Brandt, "The flux-line lattice in superconductors," *Rep. Prog. Phys.*, vol. 58, p. 1465, 1995.

[28] L. D. Cooley, G. Stejic, and D. C. Larbalestier, "Statistical variations of the elementary flux-pinning force and their effect on the shape of the bulk-pinning-force curve of high-field superconductors," *Phys. Rev. B*, vol. 46, p. 2964, 1992.